SGP-TR-180

DIRECT MEASUREMENT OF IN-SITU WATER SATURATION IN GEOTHERMAL ROCKS

Aysegul Dastan

June 2006

Financial support was provided through the
Stanford Geothermal Program under
Department of Energy Grant No. DE-FG36-02ID14418,
and by the Department of Petroleum Engineering,
Stanford University

Stanford Geothermal Program
Interdisciplinary Research in
Engineering and Earth Sciences
STANFORD UNIVERSITY
Stanford, California

Abstract

In this study we present a methodology for the direct measurement of in-situ water saturation in geothermal rocks. An experiment was designed to bring a core sample to desired pressure and saturation conditions in order to establish a steam-water environment. X-ray CT scanning was used to measure the in-situ water saturation and the porosity. In CT scanning applications for rock characterization, one of the frequently encountered artifacts is the beam hardening effect. In this work we discuss the physical reasons behind the beam hardening effect and what can be done to minimize such effects. We applied the technique on a rock sample from The Geysers rock. We present the pressure transient for a blowdown experiment on The Geysers rock and plot saturation as a function of pressure. Possibly due to beam hardening effect, however, the results deviate from what is expected. We measured the porosity of The Geysers rock to be 0.03. We present a new design for the core holder to minimize beam hardening effects.

Acknowledgments

This research was conducted with financial support through the Stanford Geothermal Program under Department of Energy Grant No. DE-FG36-02ID14418.

First of all I would like to thank my advisor Prof. Roland Horne. It takes some time for an international student to come to a different culture and a different language environment and adjust to it. Roland has always been very understanding of my situation when I was having hard time here and he always supported me. His door was always wide open to discuss anything related to courses, experiments, or anything that bothered me. I feel very lucky to have had the chance to work with him.

Dr. Kewen Li was generous to share his experience in experiments. He watched closely over me as I was working on the experimental setup and gave inspiring ideas. I also would like to acknowledge Prof. Serhat Akin, Prof Tony Kovscek, Dr. Tom Tang, and Dr. Louis Castanier for their help with the CT scanner and ideas and Aldo for doing the machinery of the apparatus and the frame.

I would like to thank my colleagues in the Stanford Geothermal Program, Allan, Anson, Egill, Rob, and Chunmei (from Supri-D). Laura Garner is also acknowledged for her administrative support.

I would like to thank my parents, brothers, and sisters and my fiancée for always believing in me and supporting me.

I dedicate this work to my brother Íkram Daştan and to my fiancée Onur Fidaner.

Contents

List of Tables

List of Figures

Chapter 1

1. Introduction

Geothermal energy is the utilization of the heat from the interior of the Earth. As a renewable energy resource, geothermal fields of the world have been utilized increasingly in the past decades. Geothermal energy offers a clean alternative to fossil fuels and its use is expected to increase in the decades to come. In a geothermal field, the cost of energy production is mostly in the initial phase when the energy plant is built. Therefore thorough characterization of geothermal fields is necessary to determine their exploitative capacity and make the most use of the fields.

In a geothermal field most of the energy is stored in the rock matrix and hot water and/or steam are used as means of transport for this energy. In such a system, knowledge of the immobile and in-situ water saturation and porosity is essential for characterization in order to make good economical analysis and for an efficient energy production. Traditionally numerical simulations based on field measurements have been used for this purpose. In-situ and immobile water saturations can be inferred from measurements of cumulative mass production, discharge enthalpy, and downhole temperature (Reyes, 2003). For that, either a zero-dimensional model based on material and energy conservation equations or a more complicated simulator like iTOUGH2 (Finsterle, 1999) can be used.

Laboratory measurements of pressure, temperature, and steam saturation can also be used to infer immobile and in-situ water saturation (Satik, 1997 and Mahiya, 1999). However for low-permeability and low-porosity geothermal rocks, this technique can be misleading (Reyes, 2003). On the other hand, direct measurement of irreducible water saturation in the laboratory would be very useful. Direct measurement involves the in-situ

measurement of pressure and water content of a rock sample at high temperature and pressure. Direct measurement allows for a direct comparison between water saturation values inferred from simulations and measured saturation values, and permits a better understanding of the geothermal field.

1.1. Earlier Work on Direct Measurement

The Geysers geothermal field is the largest producing vapor-dominated field in the world. Earlier, as part of a California Energy Commission (CEC) project, water saturation at The Geysers geothermal field has been studied (Reyes et al., 2003, Horne et al., 2003). In those works, both numerical simulations and direct measurements were made and presented comparatively. The study used an X-ray CT method for the direct measurement of water saturation in a core sample from The Geysers.

Reyes et al. (2003) concluded that the porosity of The Geysers rock is 0.03 and provided pressure vs. saturation curves at 120 ºC. According to those results, the immobile water saturation in The Geysers rock is 70%, which is much larger than, for example, a typical Berea sandstone. These results, however, were preliminary and there was just one set of measurements, which is not enough to confirm that the value is accurate. Furthermore, in that earlier work to improve the quality of the CT measurements, and in particular to reduce beam hardening effects, the sample was placed at an angle in the CT scanner. This disturbs the circular symmetry within the CT scanner and might result in aberrations in the measured CT values. Even in that configuration beam hardening was not completely eliminated. Since Geysers rock has very low permeability and porosity, it is very hard to saturate the core with water. This requires a very careful analysis as CT scans of the fully saturated and completely dried core are used as references to calculate porosity and the in-situ water saturation. Nevertheless these preliminary results were encouraging and motivate a further investigation on this technique.

1.2. Scope of the Current Work

The objective in this project is to improve and extend the direct measurement method using X-ray CT scanning. For that, we first used the same Geysers rock sample analyzed previously to repeat and then extend the measurements taken previously. Then we improved the core holder design to:

1. Accommodate two rocks for instantaneous comparison of two samples under the same pressure and temperature conditions.
2. Eliminate beam hardening effects by using a longer core and by completely avoiding the end plates.
3. Obtain multiple measurements from a rock sample at different cross sections by means of a stepper motor movement of the core.

In this work we developed a systematic procedure to characterize geothermal rocks. In this procedure, the core sample is fixed in the core holder and then the rest of the apparatus is assembled. At this point it is important to check the functionality of each component and to make sure that the system is leak free. Then the system is mounted on the CT scanner and aligned such that no beam hardening occurs. Finally the steam-water environment is established within the core and measurements are taken.

In this report we explain this procedure we developed along with the necessary background information. In Chapter 2 we give the essentials of computer tomography (CT) technique and explain how it is utilized for direct measurement of in-situ water saturation. In Chapter 3 we introduce the experimental apparatus, give information about the components used and explain how they are interconnected. In this chapter we also explain the experimental procedure to establish the steam-water environment within the core. In Chapter 4 we demonstrate and discuss the experimental results. Chapter 5 gives the conclusion and mentions future directions for the research presented in this thesis. Details of designs, some of the data, and information about the data acquisition system are given in the appendices.

Chapter 2

2. Application of Computer Tomography Technique on Rock Characterization

Computer tomography (CT) is a medical imaging technique that uses X-rays to produce images of thin slices of a desired part of the human body. The same procedure can be used to gather information about the content of rock samples. In our experiments, we used a Picker^{TM} Synerview X-ray CT scanner (Model 1200 SX), which was designed originally for medical purposes. Fig. 2-1 gives a simplified schematic of CT operation. The sample is placed within the gantry, which is a large ring as seen in Fig. 2-1. The ring contains an X-ray tube (X-ray emitter) and X-ray detectors uniformly distributed on the ring. During a CT scan, the X-ray tube makes a complete rotation around the ring. The X-ray beam is collimated to the slice of the sample being imaged. At any instant of time during the scan, this beam of X-rays is attenuated by the sample. Different parts of the beam are attenuated by varying amounts, depending on the types and amounts of material the X-rays pass through. Water-saturated rock attenuates X-rays differently than unsaturated rock. Once the different parts of the X-ray beam pass through the sample and are attenuated, their remaining intensity is measured by an arc of about 500 X-ray detectors. These X-ray measurements at the detectors are repeated hundreds of times during the scan as the X-ray tube sends X-rays through the sample at different angles.

The X-ray detectors produce electronic pulses proportional to the X-ray intensity they receive. These hundreds of thousands of data pulses, from different detectors and at different positions of the X-ray tube, are fed into a computer which uses them to form a digital image of the cross-section of the sample through which the X-rays passed. In creating the image, the computer assigns each pixel a number between -1000 and about +3000. This is called the pixel's CT number. The larger the CT number the greater the

attenuation of the material represented within that pixel and the brighter that pixel will appear in the image. By definition, air has a CT number of -1000 and water has a CT number of zero. Therefore an image of the cross-section of the image is produced. It is possible to deduce the saturation by comparing dry and saturated images of the same cross-sectional area of the sample.

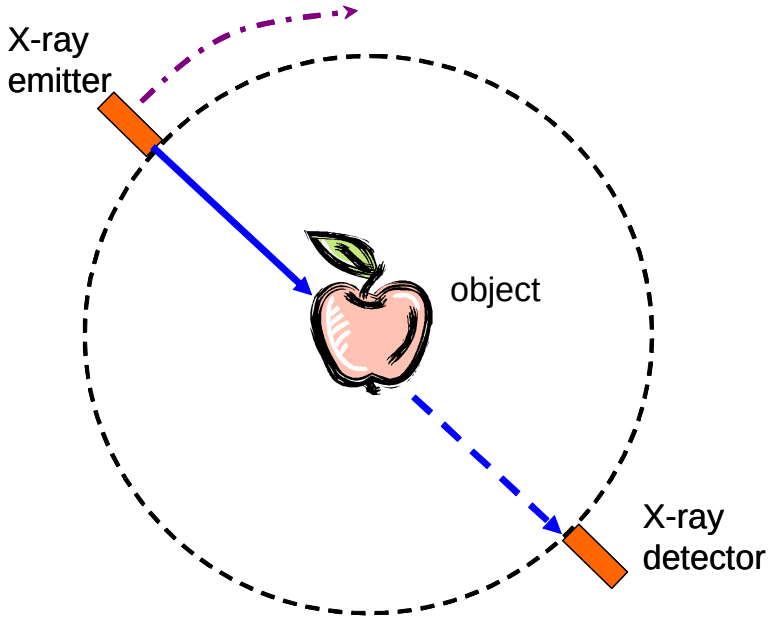

Figure 2-1: Computer tomography essentials. The object absorbs some portion of the emitted light. The remaining is detected by a detector located at the other end. There are 500 such detectors around the ring and the emitter makes a full turn at every scan. Processing of the data coming from the detectors results in the CT image.

2.1. Characterization of the Rocks: S_w and ϕ Parameters

In-situ characterization uses computer tomography (CT) images of a rock sample under various pressure and temperature conditions. Here, the objective is to determine the saturation and porosity values, S_w and ϕ respectively. CT scanner scans the sample and finds the distribution of water in the sample. Figure 2-2 shows two scans for which the core was dried and was saturated with water at room temperature. These grayscale pictures show the distribution of CT values in some cross section of the core holder. In other words, each CT number is assigned a shade of gray. Light regions have higher CT values and dark regions have lower CT values. In this example due to heterogeneity and

low porosity, it is hard to see the change in saturation by visually comparing the two images.

Figure 2-2: CT dry scan (left) and CT wet scan (right). From average values within the core, CT_{dry}=1486 and CT_{wet}=1511 are measured.

We can find the water saturation using the measured CT values by a simple analysis. $CT_{wet}(T)$, $CT_{dry}(T)$ are the CT values of the core sample when it is completely saturated by water and when the sample is vacuumed, respectively. For a physical location, the difference $CT_{wet}(T)$ - $CT_{dry}(T)$ gives a relative measure of the amount of water at that location for the 100% water saturation case. At a test condition, at the same location, there will be a mixture of water and steam; i.e., there will be less water at the location compared to the 100% saturation case. Hence, the difference between $CT_{exp}(T)$ - $CT_{dry}(T)$ gives a relative measure of the amount of water distribution at that physical location. Consequently, from Eq. 2-1 one can find the water saturation.

$$S_w = \frac{CT_{\exp}(T) - CT_{dry}(T)}{CT_{wet}(T) - CT_{dry}(T)} \qquad (2\text{-}1)$$

It is possible to measure porosity following a similar argument. For this calculation we need the CT measurements for the 100% saturation case (CT_{wet}) and the dry case (CT_{dry}). The difference between them is due to the water which fills all the pores (S_w=1). If it were not for the rock matrix, we would measure the CT number of air (CT_{air}) in the dry case and the CT number of water (CT_{water}) for the wet case. In that case, the difference CT_{water} - CT_{air} gives a relative amount of water that would fill the entire space in that

specific physical location. We can, therefore, calculate the porosity by dividing the actual amount of water, which we assume to fill all the pores in that location, by the amount of water that would fill the entire space in the location if it were not for the rock matrix (if the porosity were 1). This is formulated in Eq. 2-2.

$$\phi = \frac{CT_{wet}(T) - CT_{dry}(T)}{CT_{water}(T) - CT_{air}(T)} \tag{2-2}$$

We can apply Eq. 2-2 on the measurement given in Fig. 2-2. Using CT_{water} = 0, CT_{air}= -1000, and the measured values from Fig. 2-2, CT_{dry}=1486, and CT_{wet}=1511, we can find the average porosity to be 0.025 in this measurement. Note, however, that porosity is not the same at all locations. The spatial distribution of porosity can be found by doing the calculation for each location and then finding a distribution of porosity.

2.2. Beam Hardening Effects

Beam hardening is one of the most commonly encountered artifacts in CT scanning. Beam hardening results in a higher CT value at the edges than in the center even though the same material is used. In this section we will briefly discuss the physical reasons behind the beam hardening effect. A more detailed discussion can be found, for example in Ketcham (2001).

As explained in relevance to Fig. 2-1, X-ray CT scanning relies on attenuation of X-rays as they pass through a material. X-rays are generated by an X-ray tube. An X-ray beam generated consists of waves of different frequencies. Attenuation is modeled exponentially as given in Eq. 2-3. In this equation, α is the absorption coefficient and L is the distance traveled, I_0 is the initial energy (intensity) of the beam and I is the remaining energy after passing through the object.

$$I = I_0 e^{-\alpha L} \tag{2-3}$$

The absorption coefficient depends on the frequency of the wave. This means that different frequency components of an incident beam get absorbed in different amounts when they pass through a given length of a material. Therefore, during a CT scan, the frequency portfolio of an X-ray beam before it enters the material is different than the portfolio after it leaves the material. Usually, lower frequency beams are attenuated more, i.e., the material acts like a preferential filter. At the output although the total energy of the beam is reduced, the energy density increases. The detectors cannot detect the frequency components separately; instead they read the total power incident on them. CT number is related to the absorption coefficient α. CT scanning is actually estimating α based on input and output energies measured by the detectors, assuming they have the same portfolio of frequencies. This assumption results in a different α estimation for different lengths of the same material.

Consider two different lengths of the same material. Normally, these two should have the same absorption coefficient. However, if Eq. 2-3 is used to calculate α, for the short length we will find a higher α than the long length, meaning that the short one appears to be a more-absorbing material. Such short paths usually occur at the edges. Due to beam hardening, the edges are estimated as a more-absorbing material, and thus are assigned higher CT values, while the central locations are assigned lower CT values, although they are of the same material. Therefore, in a CT image, the edges appear brighter than the center (See Fig 2-2, for example).

Normally the absorption coefficients encountered in the human body, for which most CT scanners were designed, are smaller than the absorption coefficient of rocks. In such a case, the error margin is smaller since the overall absorption is less. In a rock, attenuation is much stronger and beam hardening usually occurs. One solution could be using a higher energy beam at the input so that the frequency portfolio of the X-rays changes less. In such a case, however, the sensitivity of detection will decrease, i.e., it will be harder to differentiate materials having slight differences in their absorption characteristics.

Beam hardening makes the choice of surrounding material extremely important. As we will discuss in the next section, we use a core holder, a coil to heat the system and insulating material around the core. As we discussed earlier, as the absorption coefficient of materials increase, beam hardening effects become more prominent. Therefore, the core holder was made of aluminum and similarly we used an aluminum coil and aluminum tapes to attach the insulating material. Stainless steel absorbs X-rays a lot more than aluminum, so its use should be avoided in the design of the core holder. In our case, the end plates are made of stainless steel, and for strength, stainless steel bolts are used to hold the end plates in place. In the scan, these steel pieces should be avoided. Also, even though aluminum is used, the core holder should be as thin as the pressure and temperature requirements permit. Figure 2-3 demonstrates the improvement achieved in the CT image quality with the second design.

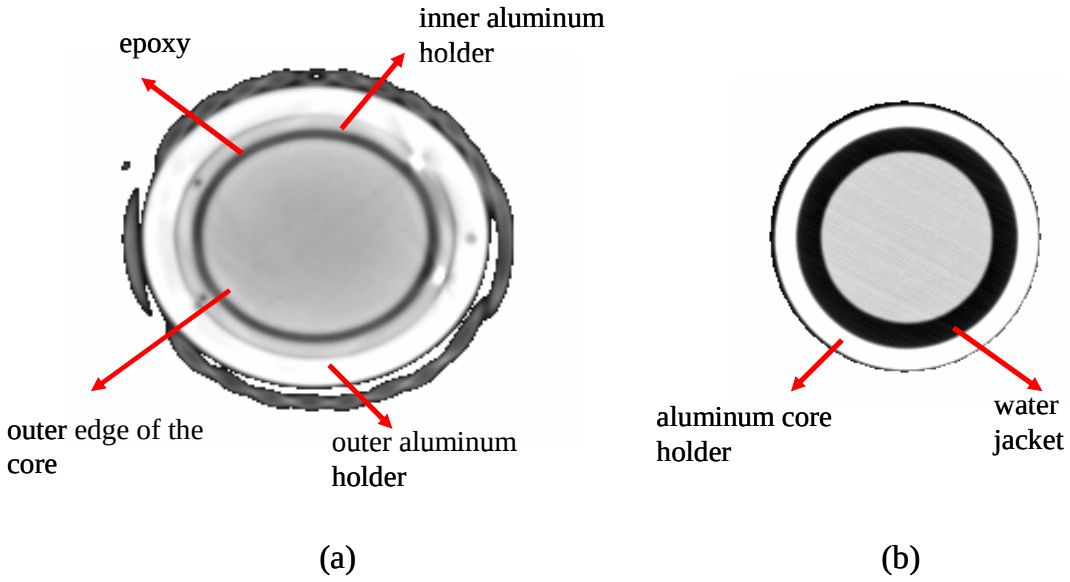

Figure 2-3: (a) CT dry scan of the initial core holder design. Beam hardening is visible around the stainless steel bolts and at the outer edge. (b) CT scan of the new core holder design. The use of a water jacket reduces the beam hardening at the outer edge of the core.

In the old design, to avoid the end plates and the stainless steel bolts, it was necessary to take the scan at an angle, disturbing the circular symmetry of the system. In Fig. 2-3 (a) the outer edge of the core is brighter than the inner portions, which is an indication of

beam hardening effect. In the new design (shown in Fig. 2-3 (b)) we used a thinner core holder and left space around the core for the water to fill in. This water jacket helps reduce beam hardening at the edge. Since water absorbs the X-rays more than air (but much less than aluminum), the effect of passing through a short path in the core is less prominent. Also having 100% water in a region allows us to check the calibration at any point during the test. We should read the same CT value, i.e., CT_{water}, within the jacket.

We will discuss core holder designs in detail in Chapter 3. We used two different core holder designs. In the second design we eliminated many of the factors that may have contributed to the significant beam hardening in the first design. Their relevance to the elimination of beam hardening will be discussed.

2.3. Mechanical Stability

If a CT scanning system is well calibrated and beam hardening effects can be eliminated, any remaining artifacts seen in the image may be due to positional instability of the object being scanned. In this section, we will explain why positional stability is important and then describe the frame we designed to fix core holders to achieve better stability.

In the beginning of this chapter, we explained the scanning mechanism. During one scan an X-ray tube is rotated and the power in the transmitted beam is detected by the detectors. This process takes about 20 seconds. Therefore, it is important to make sure that the object does not move during scan. Furthermore, since we compare CT images taken under different conditions to calculate saturation and porosity, it is essential that some physical location correspond to the same pixel in the image. It is hard to achieve this kind of short term and long term stability with the gantry only. Also the gantry itself does not have any mounts to hold the sample at a fixed location relative to the scan plane.

Figure 2-4 shows the mechanical stage we designed to improve positional stability. Since the scanning system is circularly symmetric, using a circular cross section and placing the core holder in the center of the gantry greatly improves the accuracy of the CT scanning. The height of the stage is adjustable and it is possible to align the core such that it is

centered within the scanner. The rails used on top makes it easy to move the image in the forward/backward direction. Note that it is possible to remove the top shelf temporarily to allow for the use of the original couch, if so desired. The details of this design are given in Appendix A.

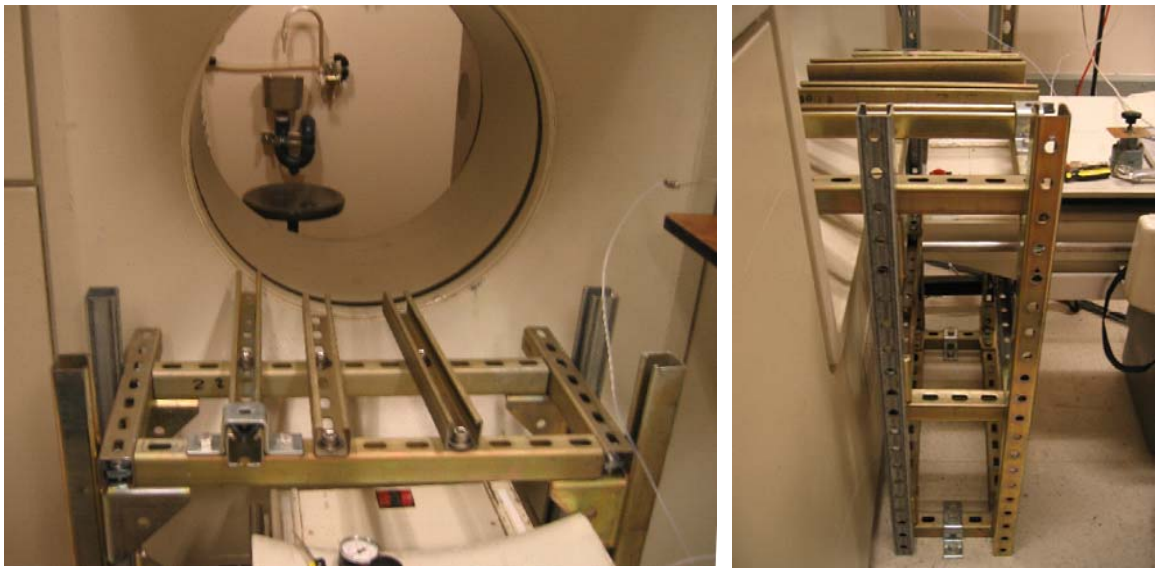

(a) (b)

Figure 2-4: Stage designed to improve stability. (a) top view (b) side view.

2.4. Calibration

Before starting to take any CT scans, it is necessary to calibrate the CT scanner. The scanner has a program to do that once the parameters of the scan are entered. We found it useful to get a scan of air after calibration. Figure 2-5 shows such a scan, and another scan taken after the core is placed. As seen, any artifact seen in the air scan is very likely to be present in the images to follow as well. It is hard to correct such errors during image analysis. Therefore every effort should be made to minimize artifacts during the initial calibration phase.

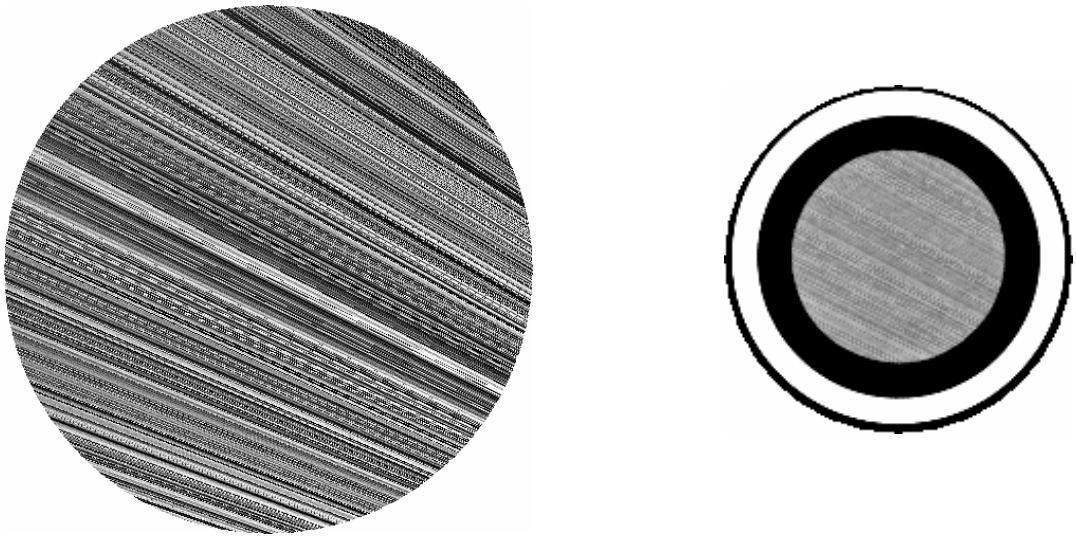

Figure 2-5: (a) CT scan of air. In this picture the color scale is such that the darkest points represent a CT value of -950 and the brightest points represent a CT value of -1050. (b) In the actual image, we see traces of the artifact present in (a).

2.5. CT Scanner Settings

Before each set of measurements some settings have to be made to optimize the scan conditions for the rock sample. Table 2-1 gives an example of the protocol information used with the Picker 1200 SX CT scanner.

Table 2-1: Protocol information used in one of the sets of scans in the Picker 1200 SX CT scanner.

PROTOCOL	1 AYSEGUL ADULT BRAIN MAS:875
PILOT SCAN	OFF (OFF/VERT/HORZ)
ORIENTATION	HEAD (HEAD/FEET)
IMG MATRIX	512 (216/512)
SCAN ANGLE	360 DEG (230/360/398)
THICKNESS	6 MM(1-10)
IMG ALGORITHM	4 (1-16)
KV	125 KV (100-140 BY 5)
FOCAL SPOT	AUTO (LARG/SMAL/AUTO)
X-RAY FILTER	C (C, 1-3)
DYN REF	ON (ON/OFF)
FIELD SIZE	48 CM (6-48)
ORIENTATION	SUP (SUP/PRN/DQR/DQL)
SAMPLING	1024 (512/1024)
SCAN TIME	4 (1-12)
COUCH INDEX	0 MM (-50 TO 50)
RESOLUTION	HIGH (NORM/HIGH/UHR)
MA	140 MA (5-200 BY 15)
ANODE SPEED	HIGH
FAST PROCESS	OFF (ON/OFF)
DYN CAL	ON (ON/OFF)

Chapter 3

3. Experimental Apparatus and Testing Procedure

The experimental apparatus is used to bring the core to the desired temperature and pressure conditions and to inject or drain water as necessary. In different phases of the experiment we used different rocks and different core holder designs. These will be discussed later in this chapter. For these different core holders the rest of the setup was the same. Fig. 3-1 shows the schematic of the experiment, which consists of the core holder, an oil bath that is connected to a coil around the core holder, pressure transducers, thermocouples, and a regulator. A vacuum pump and a water pump are also used to dry the core and inject water in the initial phases of the experiment.

The temperature is maintained by an oil bath. The oil at a controlled temperature is passed through an external aluminum coil around the core holder. On the other hand, the pressure level of interest is achieved by first pressuring the system up to the maximum pressure, typically 30-40 psi. This level is achieved using the water pump. During the course of the experiment, the pressure is gradually reduced using a regulator. This way it is possible to get measurements at different pressure and temperature conditions. Up to three pressure transducers are used for in-situ pressure measurement. As seen in Fig. 3-1, the 125 psi transducer can be optionally used for a direct measurement of the differential pressure across the core. This is especially useful if a pressure pulse decay measurement is considered to deduce system characteristics from transient data. Additionally, a 100 psi pressure gauge can be inserted for a reference reading, which can be useful to test the calibration of the transducers. Four thermocouples are used to measure the temperature at the core input (Thermocouple #4 in Fig. 3-1) and output (Thermocouple #2 in Fig. 3-1) and at two other locations outside of the core holder (Thermocouples #1 and #3 in Fig. 3-1). Transducers and thermocouples are connected to a PC for data logging.

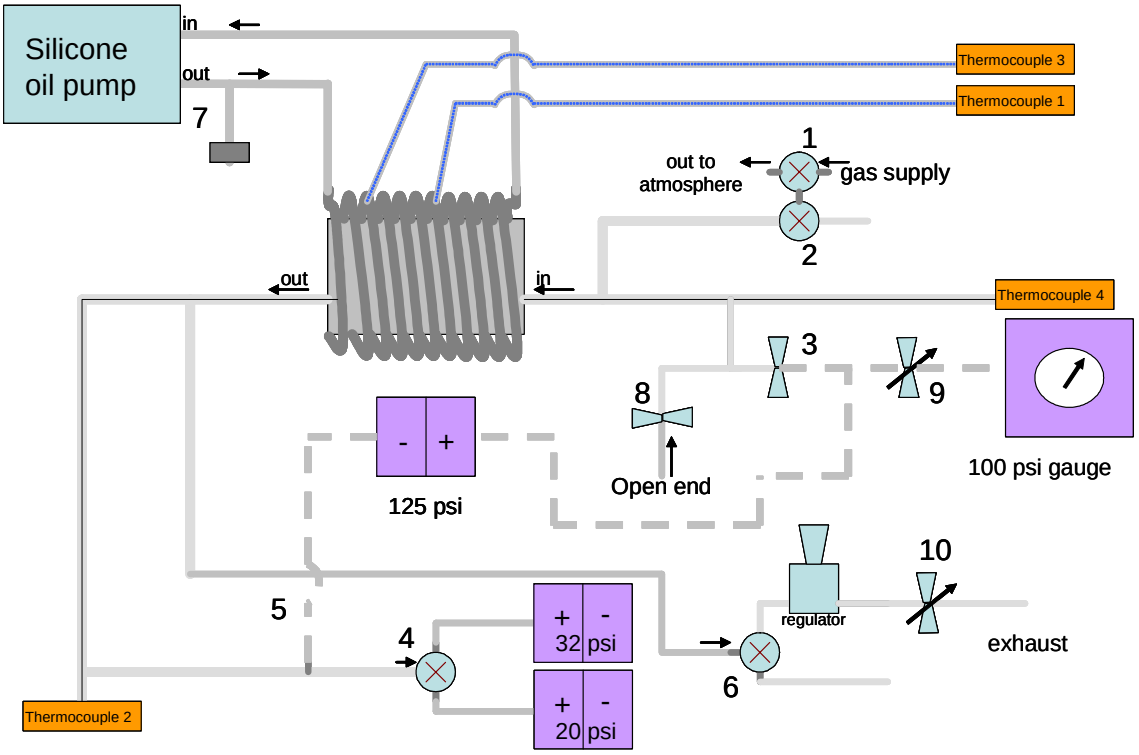

Figure 3-1: Schematic of the apparatus. 125 psi transducer can be used optionally to directly measure the differential pressure between the input and the output of the core. Similarly, the 100 psi gauge can be inserted for analog reading and calibration.

The vacuum pump (not shown in Fig. 3-1) is used to remove the air in the system before water injection. In this way, a steam-water environment can be established.

3.1. Core Holder

A good core holder design is essential to achieve good measurements. In the design, there are a number of constraints that have to be met. The core holder has to withstand the temperature and pressure conditions. Moreover, the circular symmetry of the CT scanner requires that the core holder be circular in cross section. All of the materials used have to be transparent to the X-rays used by the CT scanner. Furthermore, the core has to be fixed in the core holder so that its position does not change during the measurement.

Figure 3-2 shows the initial design for the core holder. The core is machined and inserted in an aluminum cylinder filled with high-temperature epoxy, which is then cured at 160 °C. This fixes the core in the core holder. After curing, the epoxy can withstand the temperatures and pressures used during measurements. The end-plates (not shown in the picture) are screwed in the bolts and the O-ring seals the core holder.

Using epoxy seals the core such that the flow is only from one end-plate to the other. However, the epoxy is not very robust. In time, as a result of heating and pressurizing the system up and down, cracks occurred in the epoxy. This created an alternate path for fluid flow. Especially for a low-permeability rock like Geysers, these cracks made it hard to saturate the core, possibly due to trapped gases inside. Also, using epoxy makes it very hard to use the same core holder again for other rocks. We used this design for our initial experiments with the Geysers core. However, we designed another core holder to measure the Berea sandstone and the Geysers rock together. This second design allows for direct comparison of the Berea sandstone, which is a standard characterization rock, and the Geysers rock under the same pressure and temperature conditions. In the second design, it is possible to take multiple X-ray cross section measurements without any beam hardening. Also, since a thinner core holder material is used, the images are clearer.

Figure 3-3 shows the second design for the core holder. This core holder can accommodate up to two rocks. This makes it easier to obtain measurements for two rocks at the same time. In this design, as opposed to the first case, no epoxy is used. The sides of the rocks, which were sealed by the epoxy in the earlier design, are now left open. This allows the water to enter the core not only from the front and back ends, but also from the sides. In this design, to hold the rocks in the center of the rock, flexible supports are attached on one of the rocks as seen in Fig. 3-3.

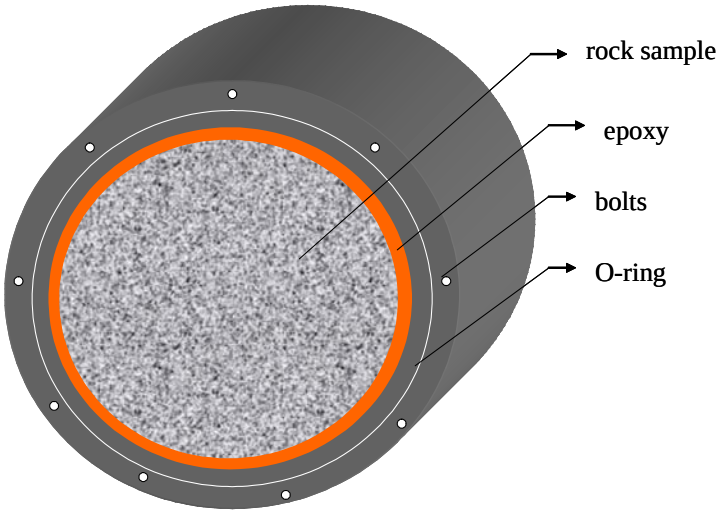

Figure 3-2: Initial core holder design for the Geysers rock

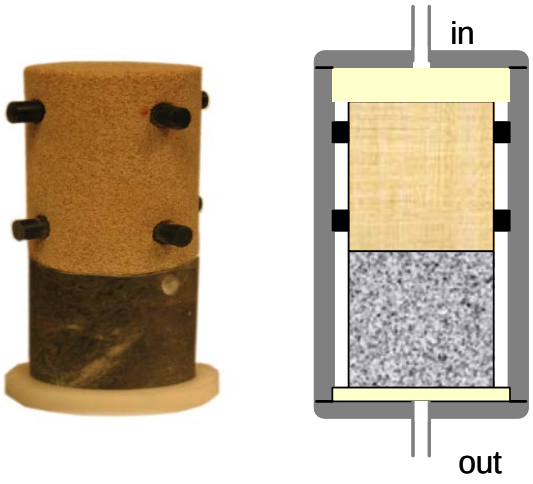

Figure 3-3: Second core holder design for the Geysers rock and the Berea sandstone. In this design water surrounds the rocks during injection.

The sandstone was fired at 790 ºC overnight before use (Shaw et al., 1998). This was done in order to deactivate the clay that would otherwise swell and fill the pores during the first water injection. Since the Berea sandstone has much higher porosity than the Geysers rock, the injection was done from the Berea sandstone side as shown in Fig. 3-3.

In both core holder designs, temperature is maintained by a silicone oil bath. Heated oil passes through a coil around the core holder. To minimize heat losses, the core and the coil around it are wrapped with insulating material. To hold the insulating material in

place, aluminum tapes and foils are used for they are both transparent to X-rays and are resistant to heat.

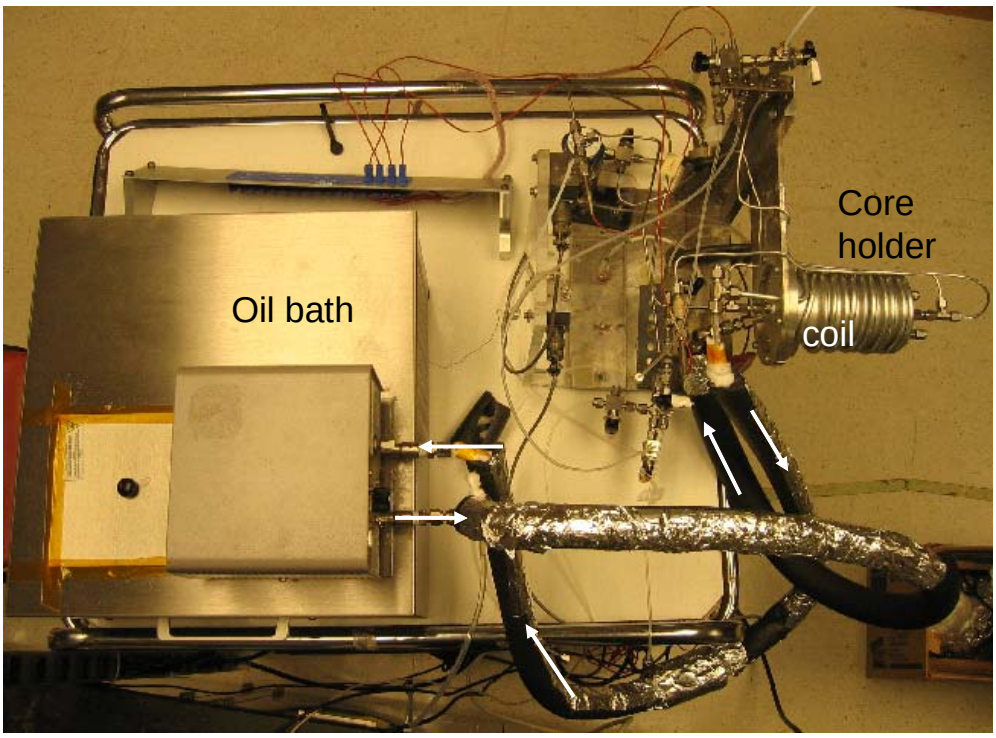

Figure 3-4: Coil around the core holder and its connection with the oil bath.

Figure 3-4 shows the coil around the core holder and the oil bath. In the heating system it is very important to insulate both the core holder and the pipes connecting the coil to the oil bath. In order to obtain a temperature of 120 ºC within the core, we had to heat the oil up to 160 ºC. Thermocouples are used to measure the temperature within the core holder. Figure 3-5 shows the insulation material wrapped around the core.

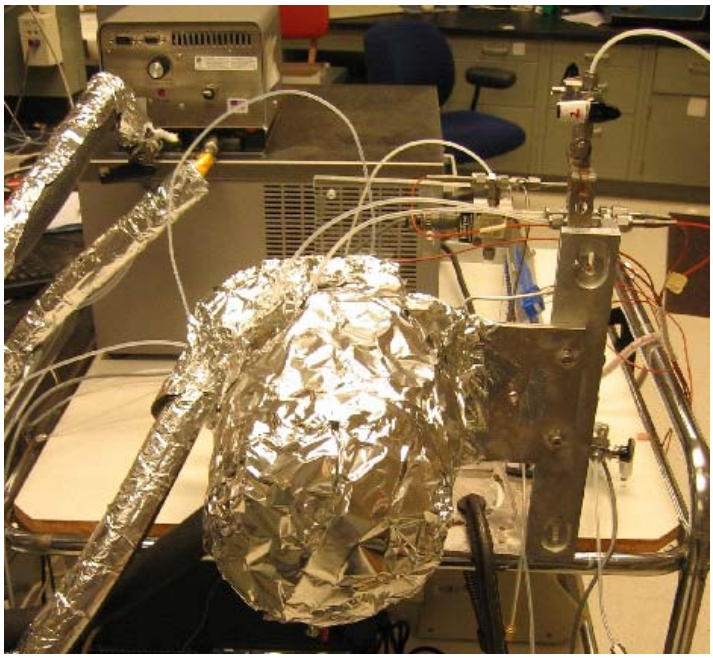

Figure 3-5: Core holder after the insulating material is wrapped around.

3.2. Pressure Transducers

Pressure transducers generate a voltage or a current proportional to the pressure they measure. Fig. 3-6 shows the electrical circuit diagram of a pressure transducer. There is a pipe connection that opens to a diaphragm. Behind the diaphragm is a variable resistor that is used as the sensing device. The diaphragm protects sensor elements from the fluid being measured. The resistance of the variable resistor is changed with the amount of strain that the diaphragm places on it. Hence, by sending a constant current through that resistor, one can monitor the voltage across it to measure the pressure. This voltage reading is then transmitted to a computer and is multiplied by an appropriate factor to get the pressure. Therefore, calibration is essential in such a pressure measurement. For calibration, typically the same pressure is measured simultaneously with a calibrated pressure gauge and the corresponding factors are found. It is important to check the calibration of the transducers from time to time.

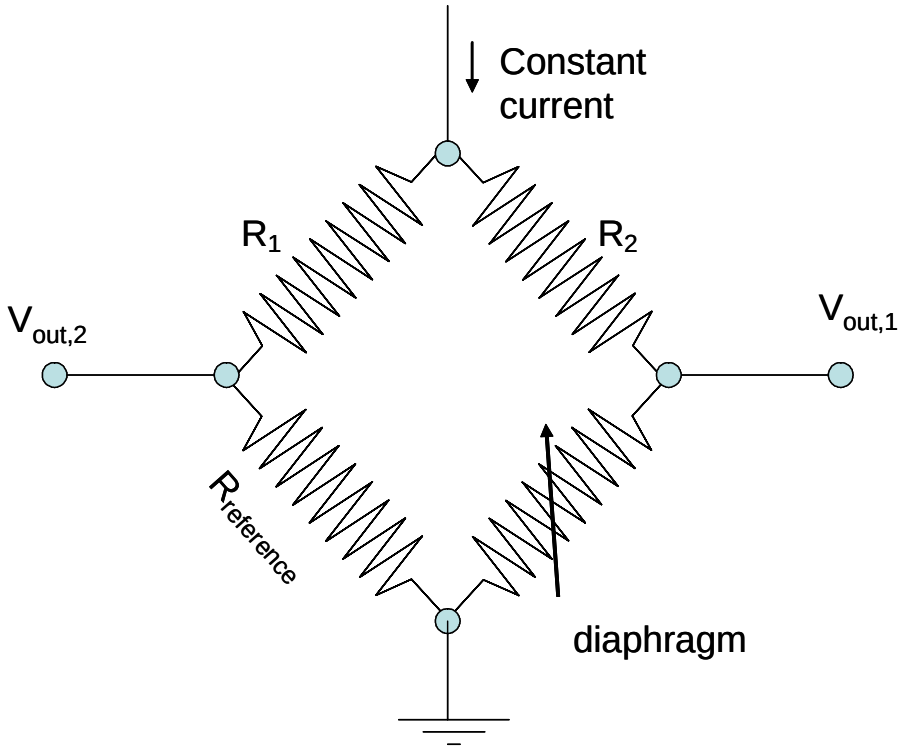

Figure 3-6: Electrical circuit schematic for a pressure transducer. The strain on the diaphragm changes the resistor value. Consequently this changes the output voltages. The voltage changes with the pressure linearly.

3.3. Other Components

The oil-heating system was manufactured by VWR with model number 9401. Depending on the temperature range desired, there are different oils that can be used to heat the system. The current one is optimized for temperatures between 100 °C and 200 °C. The temperature control feedback system does not always work properly for temperatures below 60 °C such that the temperature keeps increasing. Therefore it is necessary to check the system frequently when it is heating up. Also, it is very important to eliminate heat losses on the lines from the oil bath to the coil. We used an insulating material to wrap the pipes to minimize heat losses when the heated oil is transferred to the coil around the core.

3.4. Leak Check

To be able to achieve good measurements we have to ensure that the system is leak free. In this section we will explain the procedure we use to detect leaks. Leak checks should be done prior to any other measurement.

Leaks usually occur at loose connections and malfunctioning components. It is useful to check these components prior to installing them into the apparatus, if possible. Since we use pressure transducers to log pressure data, it is necessary to test them one by one before connecting them to the system. Once it is understood that pressure transducers are leak-free and their readings are correct, they can be used to log pressure data over time to see if there is any leak in some other part of the system.

Before we start the leak test, we first make sure all the valves and connections are connected properly. Then we calibrate the pressure transducers. The pressure data can easily be recorded over long time periods using the LabView software. However, there is a possibility that the calibration shifts during this test. For that, in the setup configuration we also include an additional manual pressure gauge on the same line with the transducer in order to cross-check the validity of the transducer reading. At the beginning of the test, we pressurize the system with nitrogen. We set the initial pressure to some value close to the maximum value allowed by the transducer.

At this point, it is important to check if there is any obvious leak in any of the connections. To detect gas leaks Snoop liquid leak detector can be used around the connection areas. It is a specially formulated liquid that adheres to vertical surfaces. Gas leaks produce bubbles, indicating the leak locations. Such leaks can generally be fixed by tightening the connections. However, in some cases, it may be necessary to replace parts.

If the decrease in pressure cannot be eliminated using the Snoop detector, it may be useful to immerse the setup in water. In this case air bubbles originating from some location travel all the way to the surface of the water and so it is much easier to locate the leaks. Indeed, immersing the components in water is the only way to understand if there is a

leak in the core holder. Therefore, it is good practice to test the core holder by itself once the core is fixed in it. Only after that should it be connected to the system. Fig. 3-7 shows a picture of the setup after it was immersed in water. Note that in such a test there are some items that need to stay away from water. The thermocouples are resistant to water; however their electrical ends need to be kept outside. A Ziploc bag was used to isolate the electrical connections from water. Similarly it is not appropriate to immerse the manual pressure gauge or the transducer in water. However, we placed them such that their valve connections, i.e., possible leak locations, are in water, as seen in Fig 3-8.

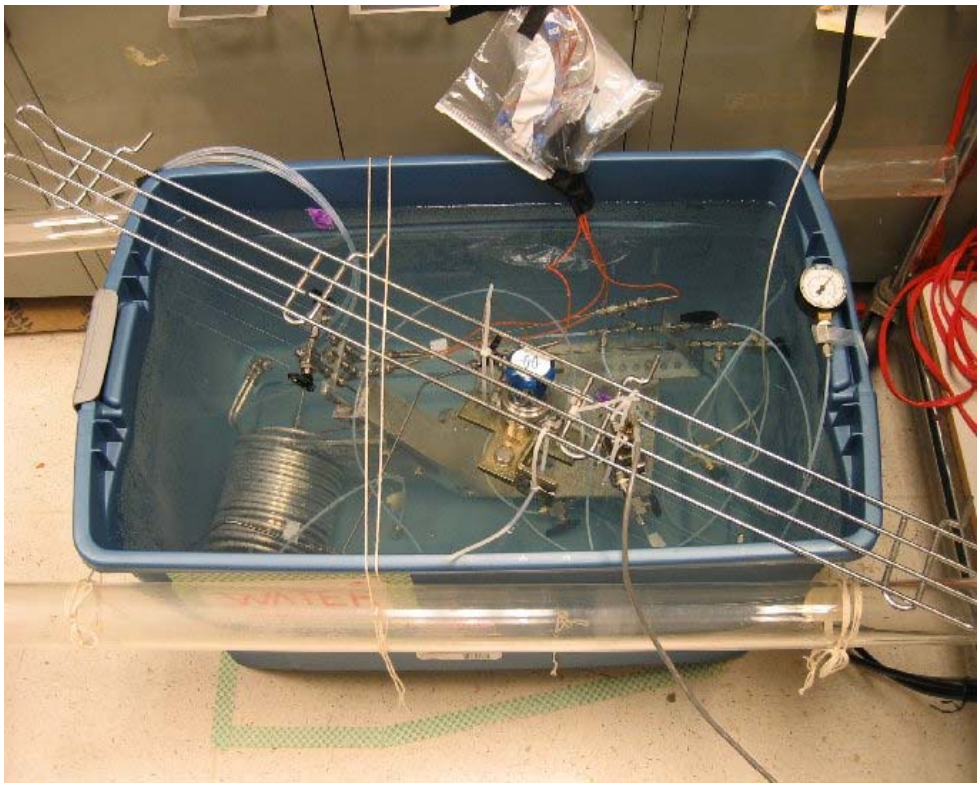

Figure 3-7: Setup immersed in water for leak test.

If the pressure drop continues despite the elimination of all noticeable leaks then one should suspect the leak might be from the parts of transducers that are left outside of the water. Sometimes an O-ring is not compressed enough to provide enough sealing or the diaphragm needs to be replaced.

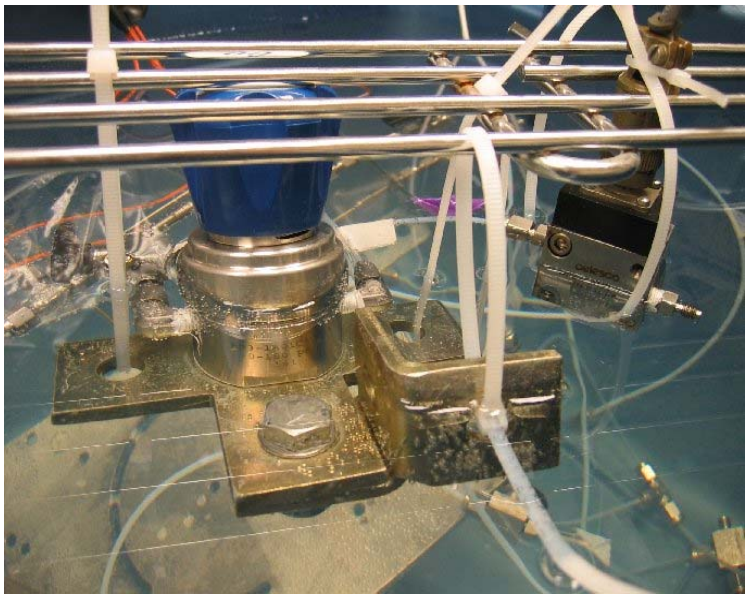

Figure 3-8: Pressure transducers and valves are outside of the water, while their pipe connections are immersed in water to observe possible leaks.

Note that a pressure drop can be observed even there is no leak at the system. This is due to the low permeability of the rock sample. It takes some time, sometimes on the order of hours, for the gas to penetrate in the rock and fill the pores of the core. Therefore after pressurizing the system, one should wait for a sufficient time before calculating the leak rate. Usually, if pressure is logged as a function of time, one sees that there is first an exponential drop and then it turns into a linear pressure drop in time. The linear portion is due to leaks in the system and the leak rate can be found from the slope of this line.

3.5. Experimental Procedure

Our aim is to measure CT_{dry}, CT_{wet}, and the CT_{exp} values that are needed to calculate the S_w and ϕ parameters using Eq. 2-1 and 2-2. In this section we describe the steps taken during a standard pressure blowdown experiment.

3.5.1. Step 1 - Drying the core

First, with all the valves open to the atmosphere, the system is dried by bringing the temperature up to 80-100 °C. This step is especially critical if there has been water

injection to the system before. Especially, for the Geysers rock porosity is very low (ϕ = 0.03) and possibly because the pores are not well connected to each other the immobile water saturation is very high. Opening the valves and heating the system vaporizes the immobile water and it can be replaced by air.

Then, the oil bath is switched off, the valves are closed and vacuum pump is connected to the system from the exhaust side, bypassing the regulator (valve #6 in Fig. 3-1). Vacuum is pulled until the pressure on the vacuum pump drops somewhere around 60-100 mTorr. This process usually takes about two days if the system has been filled with water. Also, vacuuming should be repeated when the setup is in the CT scanner, just before the first scan. In this case, however, the pressure should drop down to 60-100 mTorr level within a couple of hours. If this drop is not observed, it is worth checking the oil of the vacuum pump and replacing it if necessary. Vacuuming also ensures the system is leak-free.

At this stage CO_2 injection should also be considered for rocks with small porosity. That is because the air trapped in the pores does not let water replace it and as a result the core cannot be fully saturated. During CO_2 injection, CO_2 replaces air. When water is injected CO_2 is dissolved in water. This way the core can be fully saturated. We did not use CO_2 injection. However we were not able to saturate the core again in the initial design, after the first trial.

Once the system is dried, it is placed in the scanner. At this point one should take a couple of measurements to see if there is any beam hardening. In the initial core design, the idea was to use just one cross-section to represent the core. By placing the sample at an angle to observe a diagonal cross-section, we were able to avoid the beam hardening effect. In the second design, we took three different cross sections from the Berea sand stone and two different scans from the Geysers rock sample. Beam hardening is eliminated in this design by ensuring the end plates are far from the scanning location. In the first design, the length of the core was small, making it extremely difficult to avoid beam hardening.

During evacuation, it is important to vacuum some additional paths that are not directly connected to the main system. Some of the pressure transducers are differential pressure transducers and their positive ends are connected to the system. For a correct reading of system pressure it is important to vacuum the negative ends as well. Note, however, that this side should be leak-free, or else the pressure readings will be wrong. If this leak-free condition cannot be reasonably maintained, then that end can be made open to the atmosphere to make the reference pressure constant.

Once the system is dried, mounted on the stage of the CT scanner and aligned properly, it is ready for testing. The CT measurements taken at this point give the CT_{dry} values to be used as reference later on.

3.5.2. Step 2 - Saturating the core with water

To avoid corrosion, one needs to use deionized water for saturation. Then the flask is half-filled with water and vacuum is applied to the flask system for about half an hour. The idea here is to suck out the air dissolved in water. Then the flask is connected to the vacuumed system such that no air is let inside. This is done while the vacuum is still connected to the system. The vacuum pump is connected to valve 6 and the flask is connected to valve 1. First, valve 2 is opened to vacuum the system again (for about 40 mins). Valve 1 is then opened to let the water in. The vacuum is decoupled from the system as soon as water is observed at the output. Then, we wait until the reading on the balance carrying the flask stabilizes. This means no more water can enter the system by itself. The next step is to use the water pump to inject more water in. The water to be used with the water pump is prepared in the same way as the water used in the flask. The water pump, which is connected to valve 1, should run until the system pressure reaches 50 psi. It is important to increase the system pressure before heating to avoid steam formation as the system is heated up. It is useful to flush the system with water to ensure there is no air trapped inside the system. Figure 3-9 shows the system with the flask and the vacuum pump connected to the system.

The scan taken at this point is the CT_{wet} scan. Together with CT_{dry}, this scan serves as the reference for the in situ measurement. At this point the core is considered 100% saturated. It is important to let the water pump stay on for sufficient time to ensure that all the pores are filled with water.

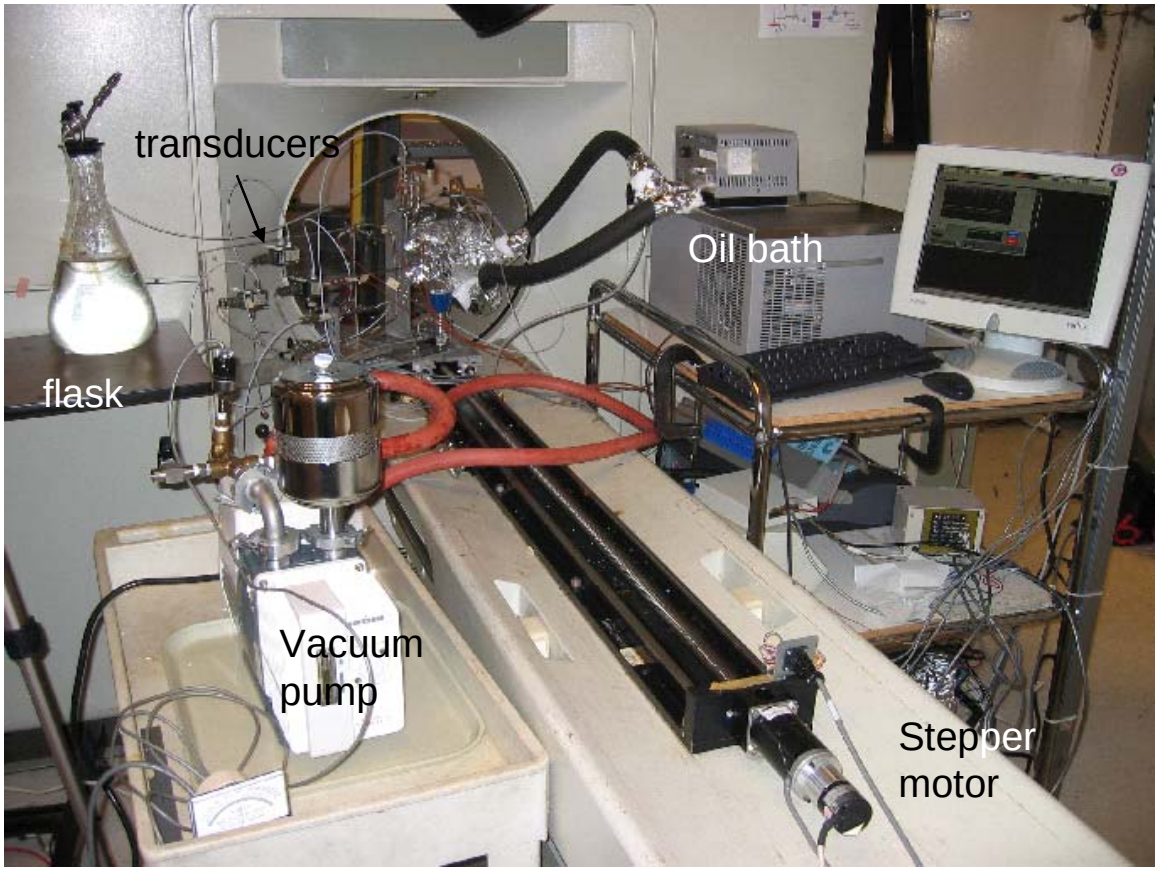

Figure 3-9: The setup in the CT scanner during initial saturation with the flask and vacuum pump connected to the system.

3.5.3. Step 3 - Heating up

The oil bath temperature is increased to 150-160 °C, as necessary to achieve 120 °C within the core. We increased the temperature by 20 °C intervals, starting from 80 °C to give the system enough time for stabilization. It is important to watch for the pressure during heat up and ensure that it is between the boiling point at 120 °C and 50 psi.

Pressures above 50 psi may result in leaks or some other failure in the system. If pressure approaches 50 psi, it should be reduced through the regulator by adjusting it properly. To avoid pressure decreasing more than intended, we also added a needle valve after the regulator (Valve 10 in Fig. 3-1). With this additional control, we were able to decrease the pressure as we planned. While heating up, we took CT scans as well to see how the saturation changed as a function of temperature.

3.5.4. Step 4 - Pressure blowdown test

After the system stabilizes at 120 °C, we start decreasing the pressure using the regulator. Once the pressure is decreased to some value, it is important to wait long enough to let the system stabilize, sometimes up to 24-36 hours. As we reduce the pressure, the system approaches the saturation pressure at 120 °C, after which some of the water will become steam and the saturation will decrease. Indeed, we expect a sudden drop in saturation at the saturation pressure. When we reach the saturation pressure from above, the fluid is all water. Then as pressure is reduced, some of the water vaporizes to keep the pressure constant at the saturation pressure, reducing the water saturation. If we continue with this, the pressure will stay constant until the immobile water saturation is reached. Since the immobile water is trapped in the pores, it cannot move out to the lower pressure regions and vaporize to keep the pressure constant. From this point on, as we open the regulator, system pressure starts to decrease again. This slowly vaporizes some of the water in the pores and the saturation continues to drop. If saturation is plotted as a function of pressure, the saturation value at the lower edge of the sudden drop at the saturation pressure is the immobile water saturation in the rock.

After atmospheric pressure is reached, vacuum is pulled to dry the system. In the end, as the pressure approaches to zero, the saturation should also decrease to the zero, which means the core dries.

Chapter 4

4. Experimental Results and Discussion

The procedure to acquire CT scans during the blowdown experiment was described in Chapter 3. In this chapter we will describe the measurements obtained based on the technique. The average CT values and the corresponding pressures are tabulated in Appendix B.

4.1. Pressure Blowdown Experiment

Figures 4-1 through 4-4 show the pressure variation during the blowdown test. The graphs are plotted with respect to time. During the experiment, the transducer readings were noisy. We did proper grounding to reduce the noise, though due to vibrations in the room, the fluctuations in the readings could not be removed completely. We used a moving average of 100 data points (data were logged every second). Figure 4-5 shows how this can remove the noise in the data.

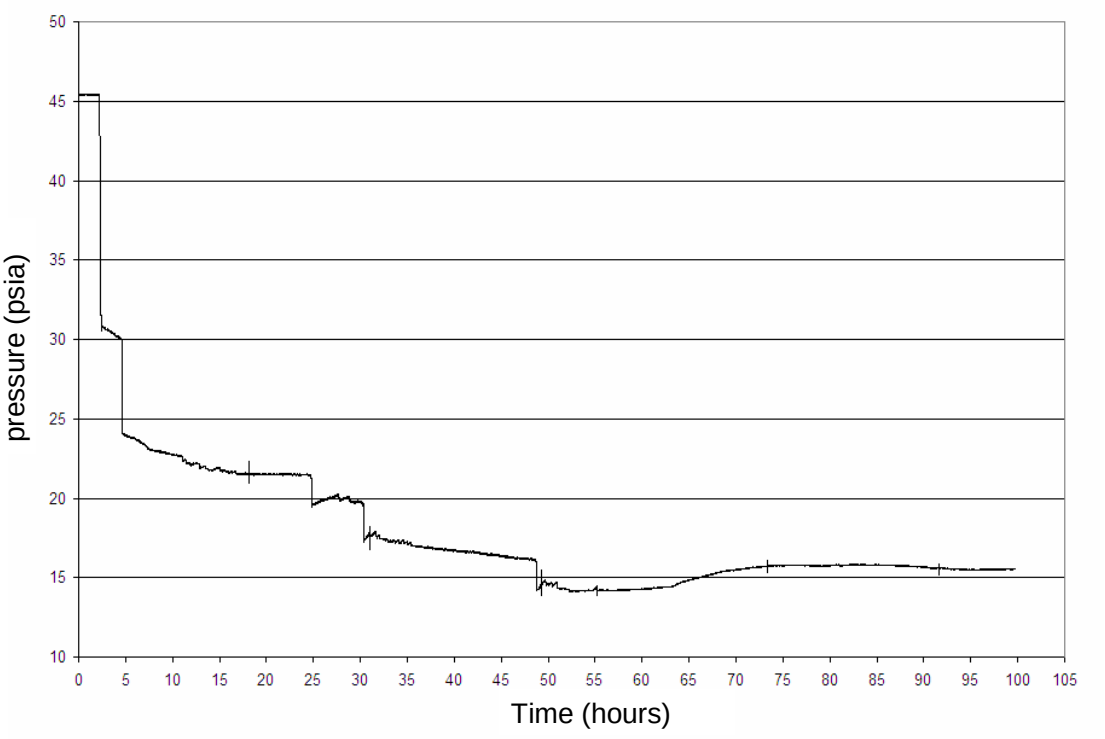

Figure 4-1: Pressure transient data – part 1.

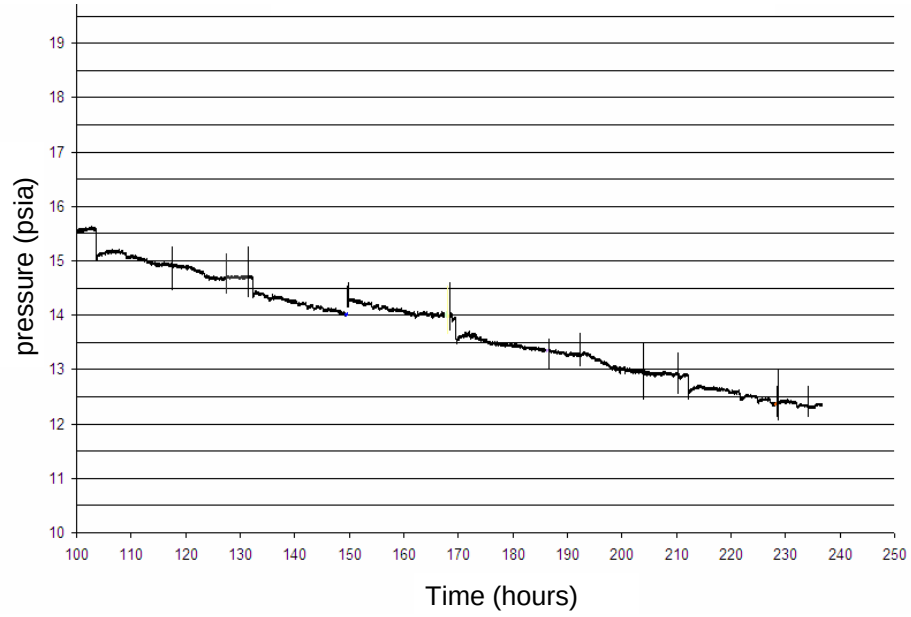

Figure 4-2: Pressure transient data – part 2.

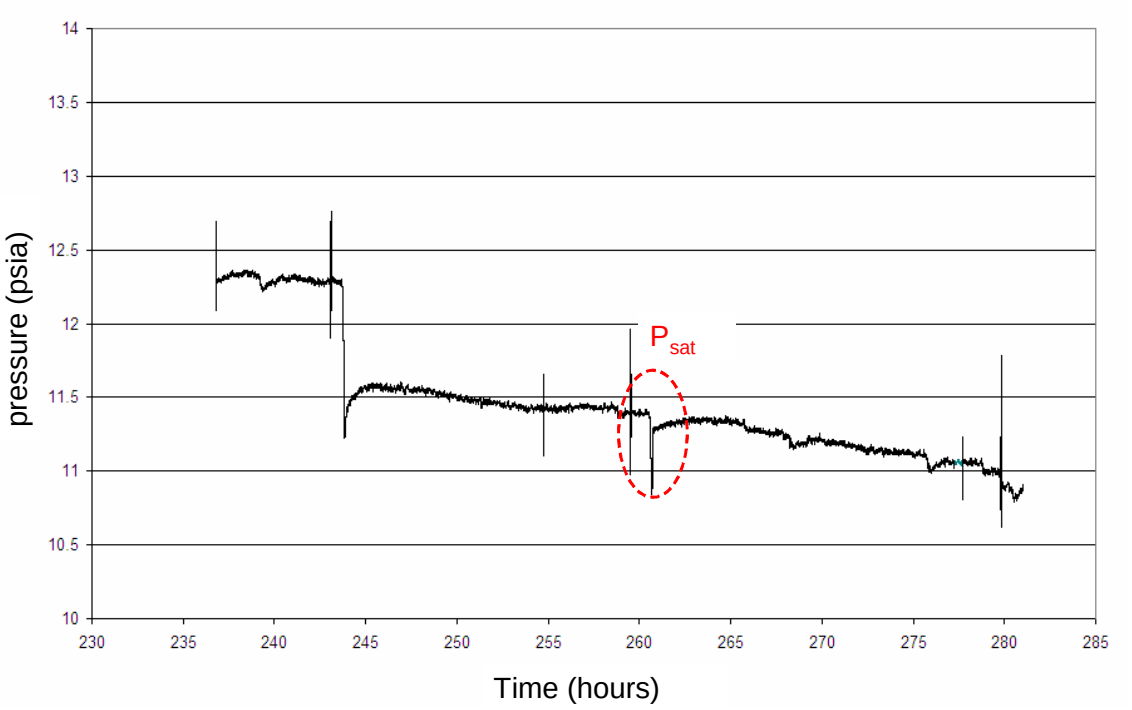

Figure 4-3: Pressure transient data – part 3.

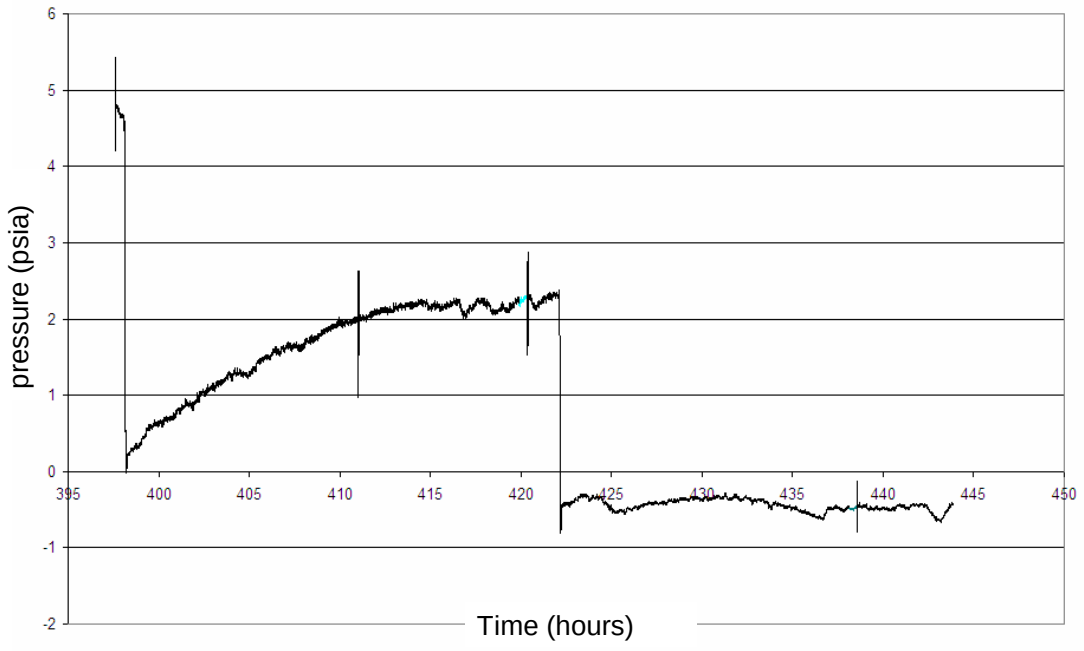

Figure 4-4: Pressure transient data – part 4.

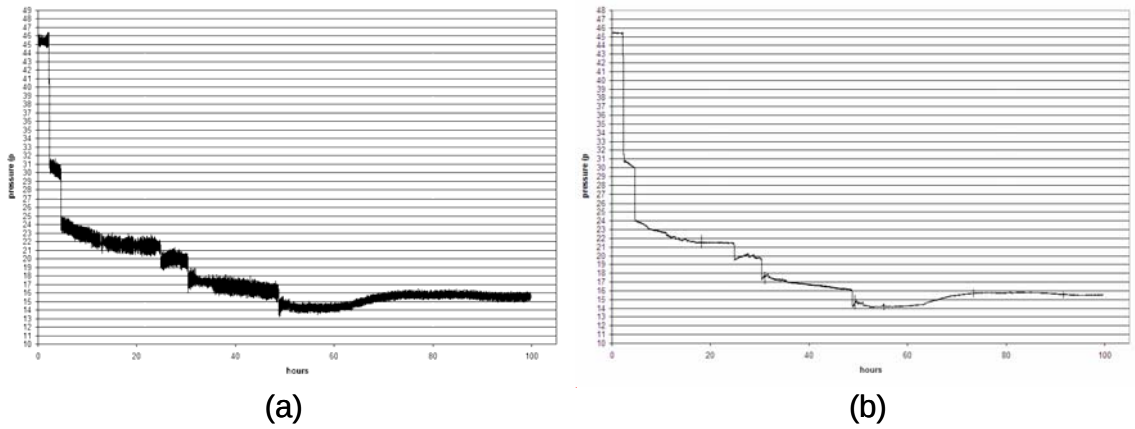

Figure 4-51: (a) original pressure data (b) noise reduction by a moving average.

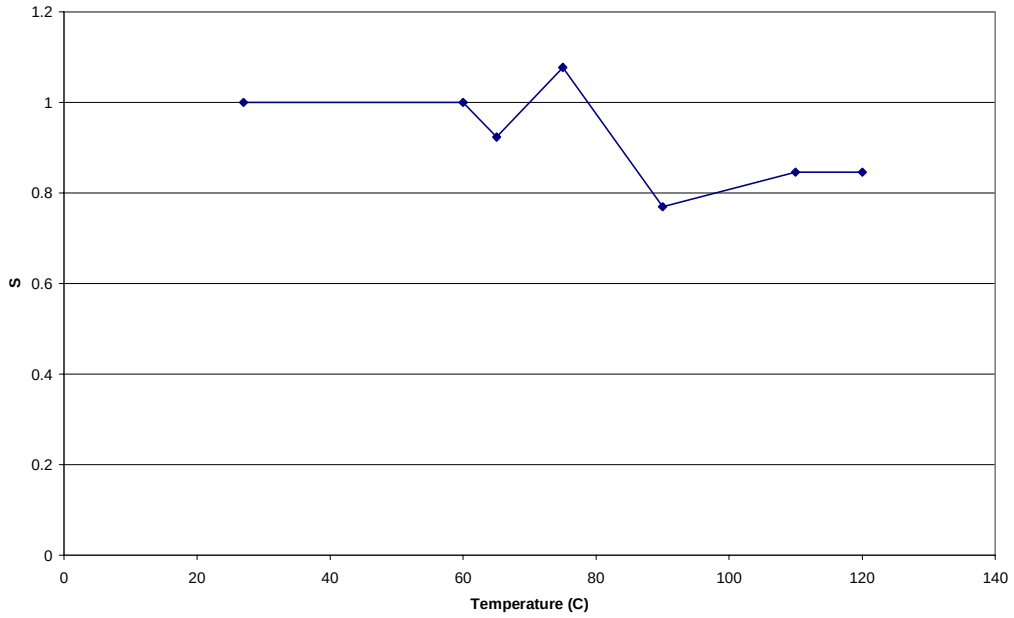

Figure 4-6: Saturation as a function of temperature.

Figure 4-6 plots saturation as a function of temperature. As temperature is increased, saturation decreases a little bit. During temperature increase, we let some water out to keep the pressure within 30-50 psi. Therefore such a decrease in saturation is expected. These data were taken without stabilization. Indeed, at that pressure the water is single phase and so stabilization does not take long. However, average CT values were used for this experiment. A variation of ±1 in average CT values may change the saturation by 5%. This should also be taken into account when this data is evaluated.

Figure 4-7 shows the saturation as a function of pressure. For this plot, only saturations corresponding to stabilized pressures are included. That is because as the pressure is decreased the system enters the two-phase region. In that region, at a certain temperature, there is a dynamic equilibrium between the liquid phase and the vapor phase. After each pressure drop, we have to wait sufficiently until the system stabilizes. From Figures 4-1 – 4-4, we see that this stabilization time can be up to 48 hours. If the system is not stabilized, the amount of water phase will change even during one scan. This will result in inaccurate saturation readings.

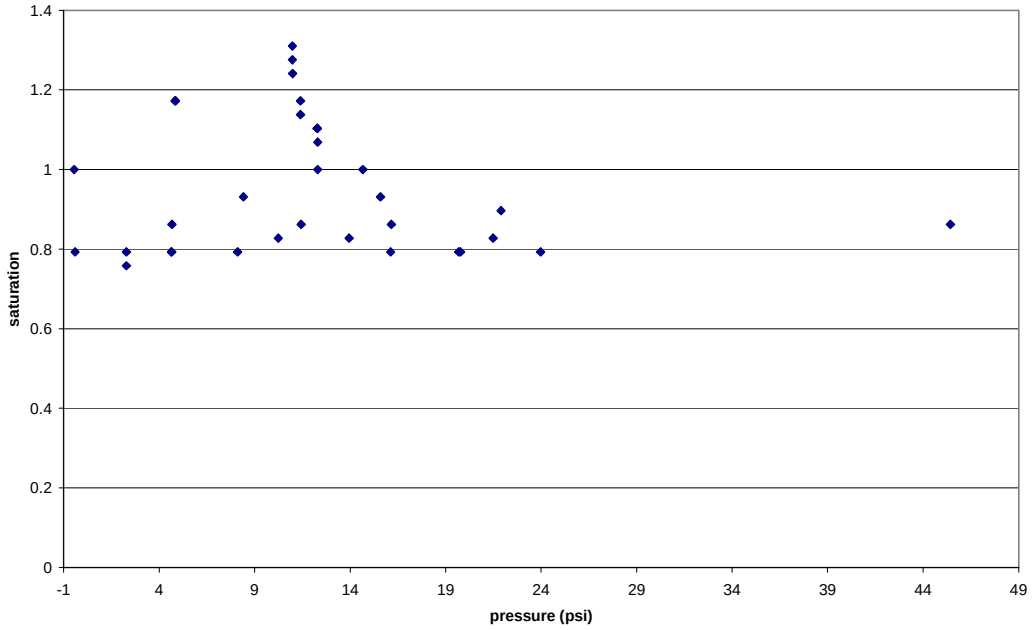

Figure 4-7: Saturation as a function of pressure at 120 ºC

In Fig. 4-7 data we do not see the kind of results we expect. Normally, we should find saturation to be constant until the saturation pressure is reached. The saturation would then drop suddenly to the immobile water saturation value and would continue to decrease as the core is dried. (This concept was discussed in Chapter 3.) We did not see that kind of behavior, but at 11-11.5 psi, we see that the system maintains the pressure although we attempt to decrease it through the regulator. This is actually the saturation pressure for this system. The saturation pressure of water at 120 ºC is 14.6 psi. Therefore,

the saturation pressure in this system is lower than expected. This could be due to a calibration shift in the transducers. However, from Fig. 4-4 we see that the system pressure remains constant at -0.5 psi after vacuum is applied for sufficiently long time. This means that the pressure calibration shifted by 0.5 psi at most during the ten days that the experiment was in progress.

The effect of saturation pressure is also visible on the pressure transient graph. In Fig 4-3, we see that after the pressure was reduced, the system increases its pressure by generating more steam. This is shown in the dashed red ellipse. Also there are multiple saturation values corresponding to that pressure in the Fig. 4-7. The reason there is ambiguity in the saturation vs. pressure graph is mostly due to our using average CT values over a large area. Due to beam hardening, as discussed in Chapter 2, this kind of analysis will not be very fruitful.

4.2. Porosity Calculations

In the results presented above, saturation values were calculated based on average CT values of the core. Since The Geysers rock is heterogeneous, it is also important to understand the spatial distribution of porosity and saturation. We analyzed images using FP Image^{TM}, a DICOM image browser. This program can process images according to scripts written by users. More information about that can be found in Appendix C. We used a script that applies Eq. 2-2 on every pixel of the image to find the porosity distribution. Fig. 4-8 shows the input dry and wet files, and the resulting porosity distribution. For these calculations the reference values CT_{air} = -1000 and CT_{water} = 0 are used. We see that there is quite a variation of porosity within the core. Moreover, we see that beam hardening effect makes it difficult to extract porosity information at certain locations.

Figure 4-9 shows the plot of the porosity variation on the horizontal axis of the cross section seen in Fig. 4-8. In Fig. 4-9 we also notice artifacts of X-ray beam hardening effect.

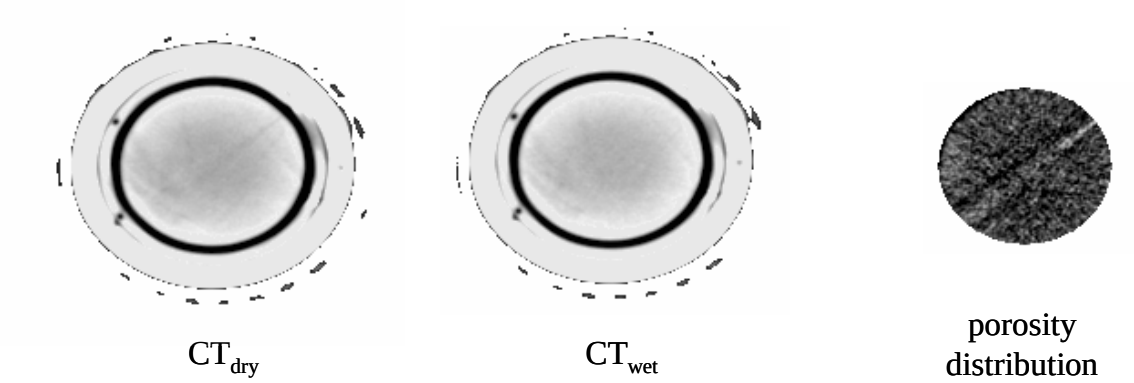

Figure 4-8: Calculation of the porosity distribution using FP Image Viewer. The 45° sloping line in the porosity distribution is an artifact of beam hardening effect. The average porosity is 0.025, but it varies throughout the cross section of the core.

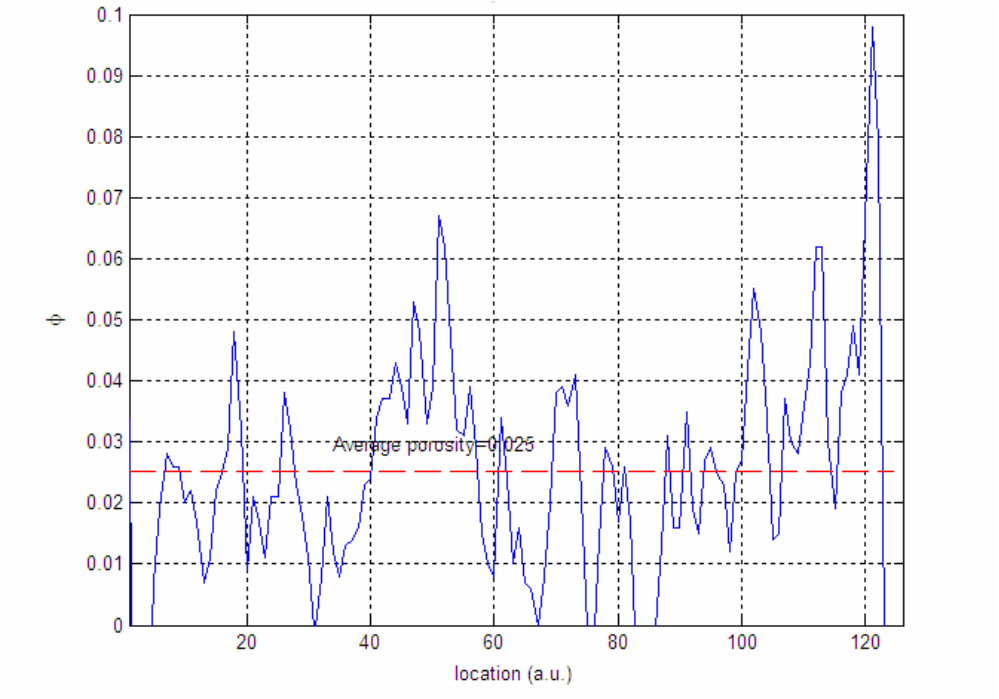

Figure 4-9: Variation of porosity across a horizontal cross section of the previous figure. (Horizontal axis is in arbitrary units.) The peak around 50 is due to the beam hardening effect.

The results presented so far were taken with the first core holder design, which, as discussed before, is prone to beam hardening effects. The second design is still under test, but it is much more promising in terms of minimizing beam hardening effects.

Chapter 5

5. Conclusions and Future Work

In this study we designed an experimental procedure for direct measurement of in-situ water saturation in geothermal rocks. We first investigated the X-ray CT scanning technique and explained some of the artifacts including beam hardening effect based on physical reasons. This let us come up with a better core holder design that would not only eliminate some of the conditions that result in beam hardening, but also allow for investigation of two rocks simultaneously.

In this work we presented and explained the steps of a blowdown test. This included methodology to find and eliminate leaks in the system. We applied this testing procedure on The Geysers geothermal rock to measure the in-situ water saturation directly. The pressure change over time was as expected. We found that the saturation pressure of the system was 11.6 psia. This is somewhat lower than the 14.6 psia value for water at 120 ºC. It could be because the actual temperature is different or due to some other experimental artifacts. Nevertheless, from the pressure vs. time graphs we conclude that we are able to maintain a steam-water environment within the core.

When we plotted saturation as a function of pressure, the result was not clear and did not follow the trend reported by Reyes et al., 2003. We believe this is due to the substantial beam hardening present in the system. In their experiment, Reyes et al. used a higher energy level in the CT scanner, which was not available to us. This is one of the reasons we observed more beam hardening. Also since the porosity of The Geysers rock is very low (~3-4%), the total amount of water within the core is small. This means that even an error of ±1 in the CT values will result in a 0.05 difference in the saturation. Therefore it is very important to eliminate beam hardening effects and correctly measure the CT

values. We designed another core holder to reduce beam hardening effects. This new core holder is still being tested.

From a comparison of the CT images of the dry sample and the wet sample, we calculated the average porosity to be 0.025 for The Geysers rock. We observed that the rock is heterogeneous and the porosity varies a lot within the core. Therefore we conclude that, for more accurate results, the spatial distribution of saturation and porosity should be taken into account.

In the near future we are planning to finish the second set of measurements with reduced beam hardening. This will give more conclusive results. Also in the new design we will be able to compare the Berea sandstone and The Geysers rock at the same time. Since the porosity of the sandstone is much higher, we believe we will be able to observe some of the phenomena including the abrupt change in saturation at the saturation pressure at least for the sandstone. This will show that our technique works in principle and that we need to find a better way to saturate The Geysers core.

It will also be useful to characterize other geothermal rocks using this technique. That study is going to result in a data base of geothermal rock characteristics that are based on direct measurements. This will help researchers working on characterization and economic assessment of geothermal fields.

Nomenclature

S_w = water saturation within the core

ϕ = porosity of the core

CT_{dry} = the computer tomography value measured when the core is completely dried

CT_{wet} = the computer tomography value measured when the core 100% saturated with water

CT_{exp} = the computer tomography value measured at an arbitrary saturation level

CT_{water} = the computer tomography value of water, usually taken to be 0

CT_{air} = the computer tomography value of air, usually taken to be -1000

α = absorption coefficient of a material

I_0 = initial intensity of the X-ray beam

I = intensity of the X-ray beam after passing through the material

L = length of X-ray beam path in a material

T = temperature

P = pressure

References

Akin,S. and Kovscek, A. R., "Computed Tomography in Petroleum Engineering Research" Application of X-ray Computed Tomography in the Geosciences. Geological Society, London, Special Publications 215, 23-38, 2003.

Finsterle, S., "iTOUGH2 User's Guide", LBNL-40040-Rev.1, March 1999.

Horne, R.N., Satik, C., Mahiya, G., Li, K., Ambusso, W., Tovar, R., Wang, C., and Nassori, H.: "Steam-Water Relative Permeability," presented at World Geothermal Congress, Kyushu-Tohoku, Japan, May 28-June 10, 2000; GRC Trans. 24, 2000.

Horne, R.N., Reyes, J.L.P., Li, K., 2003 "Estimating Water Saturation at The Geysers Based on Historical Pressure and Temperature Production Data by Direct Measurement", Final Report to California Energy Commission, June 2003.

Ketcham, R.A. and Carlson, W.D., "Acquisition, Optimization and Interpretation of X-ray Computed Tomographic Imagery: Applications to the geosciences." Computers and Geosciences, 27, 381-400, 2001.

Li, K. and Horne, R.N., "An Experimental and Theoretical Study of Steam-Water Capillary Pressure," SPEREE December 2001, p.477-482.

Mahiya G., "Measurements of Steam-Water Relative Permeability", Masters Report, Stanford University, Stanford, California, 1999.

Persoff P. and Huken J. B., "Hydrologic Characterization of Four Cores from The Geysers Coring Project" Proceedings of the 21st Workshop on Geothermal Reservoir Engineering, Stanford University, Jan 22-24 1996, p.327-333

Reyes J. L. P., Li K., Horne R N., "Estimating Water Saturation at The Geysers Based on Historical Pressure and Temperature Production Data and by Direct Measurement" GRC Transactions, 27, 715-726, 2003.

Reyes J. L. P., "Inferring Immobile and In-situ Water Saturation from Laboratory and Field Measurements", Masters Report, Stanford University, Stanford, California, 2003.

Satik C., "Experiments of Boiling in Porous Media", Proceedings of 22nd Workshop on Geothermal Reservoir Engineering, Stanford University, Stanford, California, 1997.

Shaw, J.C., Churcher, P.L., and Hawkins, B.F., “The Effect of Firing on Berea Sandstone”, SPE Formation Evaluation (Paper 18463), 72-78, 1991.

Appendix A

A. Stage Design to Improve Stability

As explained in Chapter 2, we designed a mechanical stage to improve the stability of the system and consequently achieve sharper images from the CT scanner. Figure A-1 gives the dimensions of the CT scanner. This information is essential for a good design of a stage.

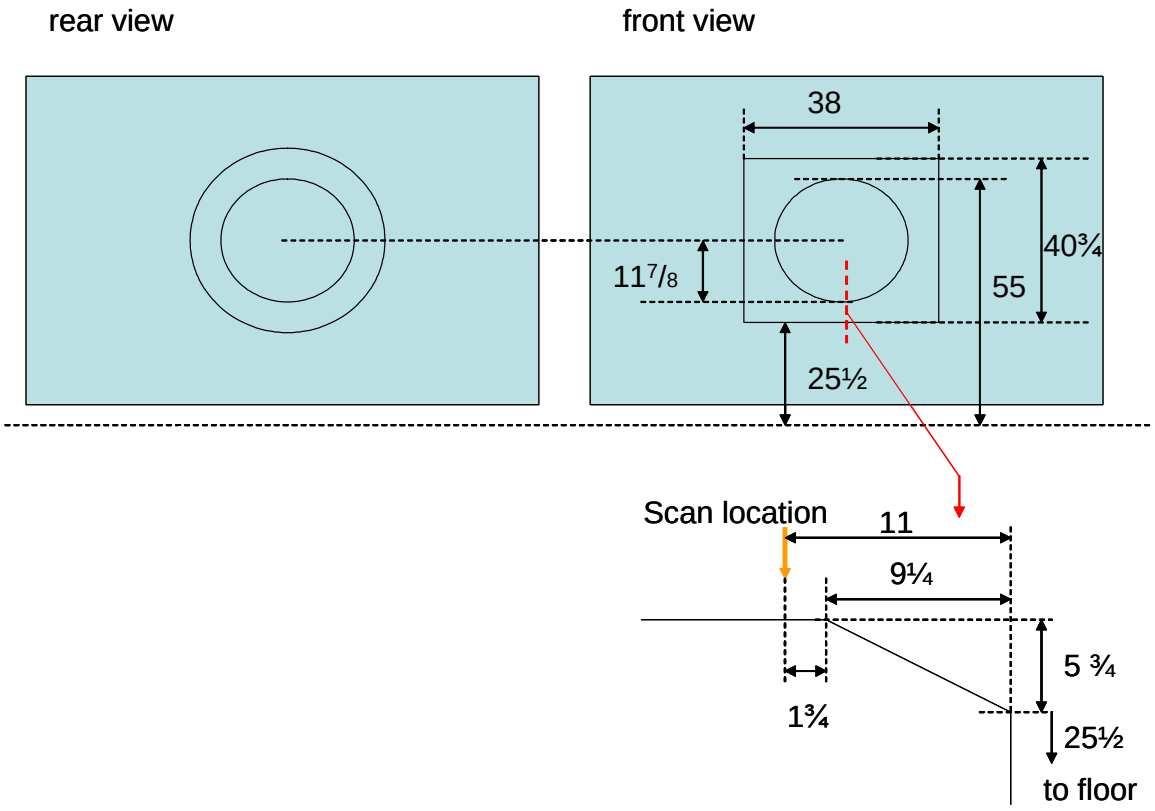

Figure A-1: CT scanner dimensions. The distances are given in inches.

We would like to center the core holder with respect to the CT scanner. Due to the circular symmetry of the system this brings improvement in the image quality. Figure A-2

shows the stage design and dimensions. We made a flexible design such that, if so desired, the original couch can still be used by simply removing the top shelf of the stage. This design can be improved by adding a motion system.

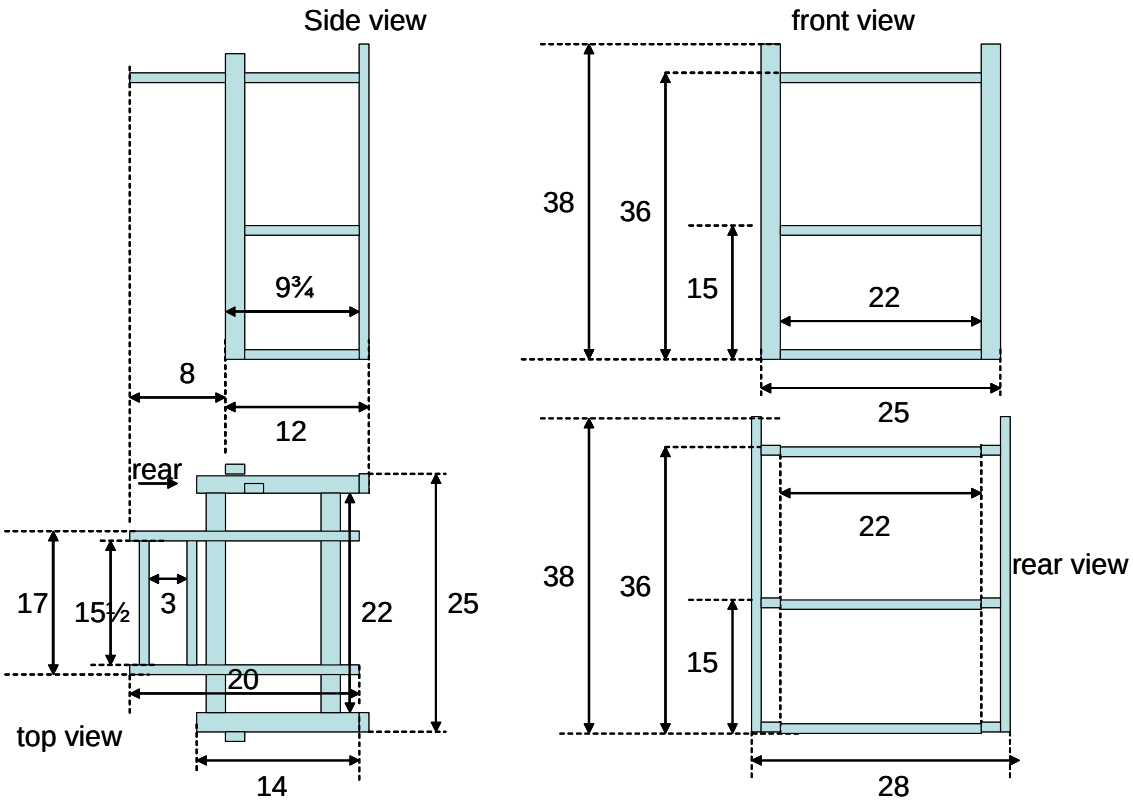

Figure A-2: Stage design. Dimensions are in inches.

Appendix B

B. Experimental Data

Table B-1: Pressure blowdown test data for The Geysers rock. The CT values listed are the average CT values within the core.

file	Date	time	Rel time (hr)	CT value	Pavg (psi)	T (C)
320.04	Aug 1st 2005	10:47	NA	1486	NA	25
320.05	Aug 2nd 2005	13:50	NA	1511	NA	25
320.06	Aug 7th 2005	18:30	NA	1515	NA	25
320.07	Aug 8th 2005	9:04	NA	1428	NA	25
320.08	Aug 10th 2005	14:44	NA	1429	NA	25
320.09	Aug 11th 2005	15:40	NA	1429	NA	60
320.10	Aug 11th 2005	17:53	NA	1427	NA	65
320.11	Aug 12th 2005	3:01	NA	1431	NA	75
320.12	Aug 12th 2005	3:11	NA	1431	NA	75
320.13	Aug 12th 2005	9:08	NA	1423	NA	90
320.14	Aug 12th 2005	12:33	NA	1425	NA	110
320.15	Aug 12th 2005	15:38	NA	1428	NA	120
320.16	Aug 14th 2005	21:40	NA	1430	NA	120
320.17	Aug 15th 2005	11:12	2.12	1425	45.42	120
320.18	Aug 15th 2005	13:32	4.44	1418	30.1	120
320.19	Aug 15th 2005	14:10	5.09	1423	23.98	120
320.20	Aug 15th 2005	22:02	12.96	1426	21.89	120
320.21	Aug 16th 2005	8:44	23.65	1424	21.48	120
320.22	Aug 16th 2005	15:08	30.05	1423	19.78	120
320.23	Aug 16th 2005	15:17	30.21	1423	19.68	120
320.24	Aug 17th 2005	9:05	48	1425	16.17	120
320.25	Aug 17th 2005	9:19	48.24	1423	16.13	120
320.26	Aug 17th 2005	9:54	48.83	1420	14.23	120
320.27	Aug 17th 2005	10:55	49.83	1423	14.55	120
320.28	Aug 17th 2005	12:50	51.75	1426	14.29	120
320.29	Aug 17th 2005	14:38	53.55	1423	14.2	120
320.30	Aug 19th 2005	12:21	99.26	1427	15.53	120
320.31	Aug 19th 2005	16:19	103.23	1427	15.59	120
320.32	Aug 20th 2005	21:12	132.11	1429	14.66	120

file	Date	time	Rel time (hr)	CT value	Pavg (psi)	T (C)
320.33	Aug 21st 2005	22:32	169.44	1424	13.94	120
320.34	Aug 21st 2005	22:45	169.67	1426	13.5	120
320.35	Aug 23rd 2005	0:16	195.18	1425	13.17	120
320.36	Aug 23rd 2005	11:27	206.36	1424	12.93	120
320.37	Aug 23rd 2005	17:04	211.98	1427	12.9	120
320.38	Aug 24rd 2005	16:14	235.14	1431	12.3	120
320.39	Aug 24rd 2005	16:15	235.17	1429	12.3	120
320.40	Aug 25th 2005	0:42	243.61	1432	12.28	120
320.41	Aug 25th 2005	0:44	243.65	1432	12.28	120
320.42	Aug 25th 2005	12:23	255.3	1425	11.43	120
320.43	Aug 25th 2005	17:35	260.49	1434	11.4	120
320.44	Aug 25th 2005	17:36	260.51	1433	11.4	120
320.45	Aug 25th 2005	18:04	260.98	1428	11.29	120
320.46	Aug 26th 2005	13:02	279.94	1434	10.89	120
320.47	Aug 26th 2005	15:34	282.48	1436	10.99	120
320.48	Aug 27th 2005	2:02	292.94	1437	11.04	120
320.49	Aug 28th 2005	1:16	316.17	1438	10.98	120
320.50	Aug 28th 2005	1:17	316.19	1437	10.98	120
320.51	Aug 28th 2005	1:18	316.21	1436	10.99	120
320.52	Aug 28th 2005	1:24	316.31	1433	10.64	120
320.53	Aug 28th 2005	1:30	316.41	1436	10.21	120
320.54	Aug 28th 2005	1:34	316.47	1437	9.88	120
320.55	Aug 28th 2005	10:54	325.81	1426	10.28	120
320.56	Aug 28th 2005	21:38	336.54	1434	10.25	120
320.57	Aug 28th 2005	21:40	336.57	1424	10.24	120
320.58	Aug 28th 2005	21:54	336.81	1426	10.32	120
320.59	Aug 28th 2005	22:13	337.12	1427	8.43	120
320.60	Aug 29th 2005	13:14	352.14	1417	8.38	120
320.61	Aug 29th 2005	13:15	352.16	1424	8.38	120
320.62	Aug 29th 2005	16:35	355.49	1432	8.43	120
320.63	Aug 29th 2005	16:36	355.51	1427	8.42	120
321.01	Aug 30th 2005	9:24	372.31	1415	8.09	120
321.02	Aug 30th 2005	9:25	372.32	1423	8.11	120
321.03	Aug 30th 2005	23:51	386.75	1434	4.86	120
321.04	Aug 30th 2005	23:56	386.84	1434	4.83	120
321.05	Aug 31th 2005	11:05	397.99	1425	4.67	120
321.06	Aug 31th 2005	11:06	398	1423	4.65	120
321.07	Aug 31th 2005	11:08	398.04	1423	4.65	120
321.08	Aug 31th 2005	11:16	398.17	1426	0.54	120
321.09	Sep 1st 2005	11:09	422.05	1423	2.29	120
321.10	Sep 1st 2005	11:10	422.07	1422	2.29	120

file	Date	time	Rel time (hr)	CT value	Pavg (psi)	T (C)
321.11	Sep 1st 2005	11:16	422.17	1423	0.045	120
321.12	Sep 1st 2005	13:04	423.97	1426	-0.31	120
321.13	Sep 2nd 2005	12:00	446.9	1419	-0.43	120
321.14	Sep 2nd 2005	12:01	446.92	1429	-0.44	120
321.15	Sep 2nd 2005	14:01	448.92	1423	-0.39	120

Appendix C

C. Data Acquisition and Image Analysis

C.1. Data Acquisition

The blowdown experiment that was explained in Chapters 3 and 4 was completed in ten days. After each pressure change, the system needed some time to come to stabilization so that we could take a new CT scan. In such a system it becomes essential to use an automatic data logging system for accurate data reading. We used the LabView™ software of National Instruments along with National Instruments SCB 68 board to log the temperature and pressure data in a computer at predetermined time intervals. We also used a web camera in the laboratory and had remote control on the lab computer in order to check data logging remotely. The convenience of remote access is especially necessary for experiments that take such a long time.

The SCB 68 board is a shielded board that can take in analog signals generated by measurement devices such as thermocouples and pressure transducers. It has eight differential and 16 single ended input channels. The analog data it takes is digitized and sent to the PC via a PCI card. LabView has access to the readings in the PCI card. These readings are properly scaled to give temperature and pressure readings. Fig. C-1 shows the graphical user interface of the program. The logged data is written in a text file along with the date and time of data arrival.

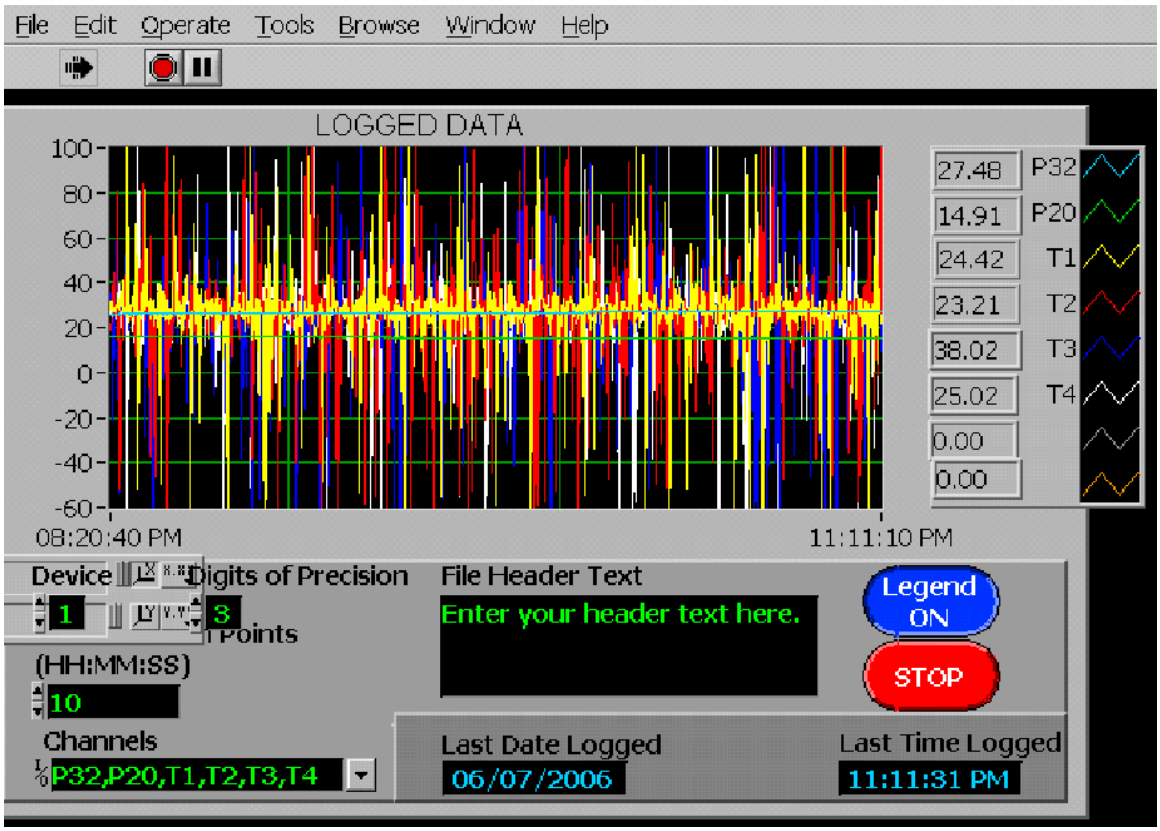

Figure C-1: A screen snapshot of the LabView program used for data acquisition.

C.2. Image Analysis

The raw data stored in the computer tomography tool has to be converted to a standardized format to be useful. We converted the data that were generated in the internal format of Picker series scanners to the format known as digital imaging and communications in medicine (DICOM). This is an established format to standardize the images obtained from medical imaging tools such as CT scanners or MRI. Once the files are in this format, a variety of image processing programs can be used to view and analyze the CT scan files. We used the software FP Image Viewer^{TM}. Writing scripts, it is possible to do certain calculations on the images. Earlier, some scripts were developed by Prof. Serhat Akin of Middle East Technical University, Turkey to be used with FP Image Viewer. Using those software it is possible to align two images such that pixels correspond to the same physical locations and to delete the irrelevant parts of the image

(i.e. anything other than the core). This helps eliminate the edges that are subject to substantial beam hardening. One of the scripts calculates and maps porosity and another calculates the saturation distribution.

Incidentally, in a CT image there is an array of CT values, each corresponding to a specific location. There is an option in FP Image to save DICOM images as text files that consist of arrays of CT values. One can use MATLAB, or any other programming environment with these text files to further process the image data.